

## Specific surface effect on transport properties of NiO/MgO heterostructured nanowires

Keisuke Oka,<sup>1</sup> Takeshi Yanagida,<sup>1,2,a)</sup> Kazuki Nagashima,<sup>1</sup> Hidekazu Tanaka,<sup>1</sup> Shu Seki,<sup>2,3</sup> Yoshihito Honsho,<sup>3</sup> Manabu Ishimaru,<sup>1</sup> Akihiko Hirata,<sup>1</sup> and Tomoji Kawai<sup>1,b)</sup>

<sup>1</sup>Institute of Scientific and Industrial Research, Osaka University, 8-1 Mihogaoka, Ibaraki, Osaka 567-0047 Japan

<sup>2</sup>PRESTO, Japan Science and Technology Agency, 4-1-8 Honcho Kawaguchi, Saitama, 332-0012 Japan

<sup>3</sup>Division of Applied Chemistry, Graduate School of Engineering, Osaka University, 2-1 Yamadaoka, Suita, Osaka, 565-0871 Japan

(Received 21 July 2009; accepted 3 September 2009; published online 30 September 2009)

NiO heterostructured nanowires are promising building blocks due to the nonvolatile resistive switching in nanoscale. Here, we report on the noncontact transport measurements of single crystalline NiO/MgO heterostructured nanowires by utilizing a microwave conductivity method. We found the substantial discrepancy up to four orders of magnitude between the heterostructured nanowires and heterothin films on the resistivity when the bulk resistivity increased, whereas the reasonable agreement was found for relatively conductive range. The origin of such huge discrepancy was interpreted in terms of both the large specific surface area of nanowires and the surface transport events of insulative NiO. © 2009 American Institute of Physics.

[doi:10.1063/1.3237176]

One-dimensional nanostructures using transition metal oxides (TMOs) are potential candidates to incorporate the fascinating physical properties, including superconductivity,<sup>1</sup> ferromagnetism,<sup>2</sup> ferroelectric,<sup>3</sup> resistive memory effect,<sup>4</sup> metal-insulator transition,<sup>5</sup> and others, into nanowire-based devices.<sup>6</sup> Among various interesting TMOs, NiO is an anti-ferromagnetic insulator, and, historically, the insulating nature, which cannot be explained in terms of a classical band model, has been intensively studied to understand the role of an electron correlation.<sup>7</sup> Other investigations as to NiO have dealt with the antiferromagnetic properties including the exchange bias effect,<sup>8</sup> sensing gases via the semiconducting properties<sup>9</sup> and the electrochromism utilizing the redox phenomena.<sup>10</sup> Recently, nonvolatile resistive switching memory effects in NiO thin films have renewed the interests in the transport properties of NiO toward the nonvolatile memory device applications.<sup>11–13</sup> Creating one-dimensional NiO nanostructures via self-assembling would be one key technological step toward nanoscale nonvolatile memory devices using NiO. However, the fabrication of NiO nanowires had been difficult and unfeasible due to the material limitation of one-dimensional crystal growth mechanisms including vapor-liquid-solid growth.<sup>14,15</sup> One of the ways to overcome this critical issue is to utilize a core/shell heterostructured oxide nanowire, since the method allows us to fabricate a wide range of oxide materials.<sup>16–18</sup> Previously, we have fabricated the MgO/NiO core/shell heterostructured nanowires<sup>19</sup> using the *in situ* formation technique newly developed.<sup>20</sup> Since both MgO and NiO have the same crystal structure (rock-salt) and the lattice mismatch is quite small (0.7%), the material combination of MgO and NiO is ideal to create the well-defined core/shell heterostructured nanowires. In addition, we have shown the existence of nonvolatile memory effects within the NiO-based heterostructured nano-

wires down to 10 nm range.<sup>19</sup> However, the knowledge as to the transport properties of MgO/NiO heterostructured nanowires is still scarce due to the inherent issues of nanoscale contacts with electrodes in the device structures. As such investigating the transport properties of heterostructured nanowires via a noncontact method would be invaluable. In this study, we investigate the transport properties of NiO/MgO heterostructured nanowires by utilizing a noncontact microwave conductivity method.

MgO/NiO core/shell heterostructured nanowires were fabricated by *in situ* laser molecular beam epitaxy technique.<sup>19</sup> The details of fabricating MgO core-nanowires can be seen in Ref. 21. The oxygen pressure and the substrate temperature during the shell layer formations were ranged from 10<sup>-3</sup>–10 Pa and RT–800 °C, respectively. After the deposition, the samples were cooled down to room temperature (RT) from the set temperature for 30 min. To evaluate the crystallinity of NiO/MgO heterostructured nanowire on MgO (100) substrate, x-ray diffraction measurement was performed. We have confirmed that NiO shell-layers were epitaxially grown on MgO core-nanowires, as reported in Ref. 19. To characterize the morphology of resultant nanowires, a field emission electron microscopy (FESEM, HITACHI S-4300) at an accelerating voltage of 30 kV was used. Prior to the FESEM observation, Pt was deposited on the samples to prevent the charging. The microstructural properties, including the crystallinity and the MgO/NiO heterointerface, were evaluated by using a transmission electron microscopy (TEM). We have confirmed (i) the smooth covering surface of MgO/NiO heterostructured nanowires by FESEM, and (ii) the well-defined core/shell interface by TEM and electron diffraction analysis, as reported in Ref. 19. Thus, the *in situ* formation technique and the crystal matching of MgO and NiO allow us to fabricate the MgO/NiO heterostructured nanowires with well-defined heterointerfaces.<sup>19</sup> To characterize the transport properties of heterostructured nanowires, a microwave conductivity measurement (MCM)

<sup>a)</sup>Electronic mail: yanagi32@sanken.osaka-u.ac.jp.

<sup>b)</sup>Electronic mail: kawai@sanken.osaka-u.ac.jp.

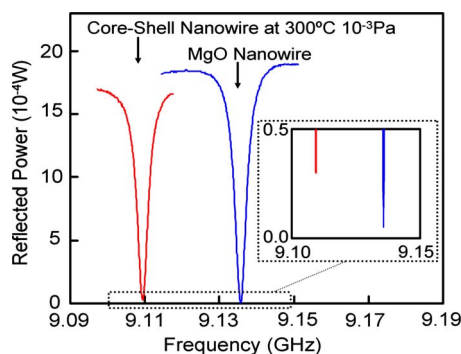


FIG. 1. (Color online) Typical resonant curves of microwave reflected powers for MgO core-nanowires and the NiO/MgO heterostructured nanowires. The inset shows the magnified data around the resonant frequency.

was performed. The microwave frequency and power were set at  $\sim 9.1$  GHz and 3 Mw, respectively, so that the motion of charge carriers cannot be disturbed by the low electric field of the microwave. The absorbed power of microwave by the samples was monitored as changes in the reflected microwave from a resonant cavity ( $Q = \sim 2500$ ) with the samples, and measured as a function of the frequency. All the above experiments were carried out at RT. The conductivity ( $\Delta\sigma$ ) of the samples is related to the reflected microwave power at the resonant frequency ( $\Delta P_r/P_r$ ) via the formula  $\Delta\sigma = (1/A)(\Delta P_r/P_r)$ , where  $A$  is a sensitivity factor. The other details of the set of apparatus were described in Ref. 22. To estimate the resistivity of nanowires from MCMs, the nanowire density and the nanowire length were analyzed by averaging the data over 500 nanowires in FESEM images for statistical reliability.

Figure 1 shows the typical resonant curves of microwave reflected powers. For comparison, the data of both only MgO core-nanowires and MgO/NiO heterostructured nanowires were shown in the figure. The observed resonant frequency shift for the heterostructured nanowires is due to the change of the dielectric constant. As shown in the inset figure, the  $Q$  factor for the heterostructured nanowires was significantly larger than that of MgO core-nanowires. This indicates that the conductivity of heterostructured nanowires is much higher than that of MgO core-nanowires. Thus, the microwave conductivity technique is capable of detecting the transport properties of heterostructured nanowires without any electrodes and the related contact issues. Figure 2 shows the resistivity of the MgO/NiO heterostructured nanowires when varying the oxygen pressure during shell layer forma-

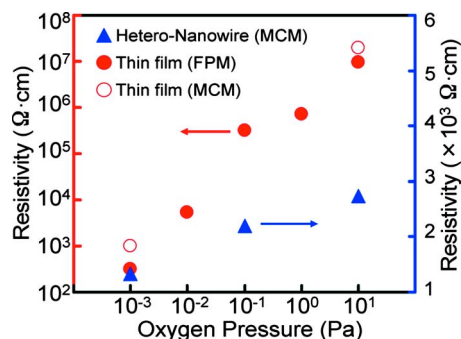


FIG. 2. (Color online) Resistivity data of the NiO/MgO heterostructured nanowires and NiO/MgO heterothin films when varying the oxygen pressure during NiO layer formation under 300 °C. The data of both MCMs and FPMs were shown in the figure.

tion under 300 °C. For comparison, the four-probe measurement (FPM) data of MgO/NiO heterothin films were shown in the figure. There are three major trends in the transport data. First, the resistivity of both heterostructured nanowires and heterothin films increased with increasing the oxygen pressure. In fact, this trend is completely opposite when compared with the trend of the bulk  $p$ -type conduction mechanism.<sup>7</sup> Previously, we have identified that the conductivity of the low temperature grown NiO strongly correlates with tailing the band edge via the deterioration of crystallinity.<sup>23</sup> Thus, the oxidization effect on the conductivity is common in both heterostructured nanowires and thin films. Second, the resistivity of both heterostructured nanowires and heterothin films were nearly identical for low oxygen pressure range  $10^{-3}$  Pa, indicating that the NiO quality should be similar for both systems. Third, the discrepancy between the heterostructured nanowires and the heterothin films tended to be larger as the ambient oxygen pressure tended to increase. At the highest oxygen pressure, 10 Pa, the resistivity of heterostructured nanowires was four orders of magnitude lower than that of heterothin films. In fact, this discrepancy differs from the case of MgO/titanate heterostructured nanowires, where both heterostructured nanowires and heterothin films showed similar resistivity trends.<sup>20</sup>

Here, we question the origin of such huge discrepancy in MgO/NiO heterostructures. There are several possible scenarios to explain the discrepancy. First, the difference between the microwave conductivity (ac) measurements and the FP (dc) measurements might cause the discrepancy via the frequency dependence of carriers. Thus, we examined the validity of the MCMs by comparing with the FPM data for MgO/NiO heterothin films grown under 300 °C and  $10^{-3}$  – 10 Pa. The data are shown in Fig. 2. Clearly both data are comparable, and at least the frequency dependence alone cannot explain the observed discrepancy in four orders of magnitude. In fact, this agreement is theoretically understandable when using relatively low mobility materials including oxides, since the hole mobility of single crystalline NiO at RT was reported to be  $35 \text{ cm}^2 \text{ V}^{-1} \text{ s}^{-1}$ .<sup>24</sup> Second possible model assumes the drastic degradation of crystallinity for entire NiO shell layers of heterostructured nanowires in comparison with the heterothin films. In this scenario, the “entire” NiO shell layers must be strongly deteriorated. Although our TEM analysis could not identify such crystal degradations, this scenario cannot be excluded by considering the degree of the crystal degradations and the effect on the transport properties. Third model is based on the large specific surface area effect on heterostructured nanowires compared with heterothin films. The specific surface area of heterostructured nanowires can be estimated to be approximately four orders of magnitude larger than that of heterothin films. If the crystal disorders naturally occurred at surfaces and/or interfaces introduce mobile carriers,<sup>25</sup> the third model can explain the discrepancy between the heterostructured nanowires and the heterothin films on the transport. It is noted that the major difference between the second model and the third model is either “bulk” effect or “surface and interface” effect. In the third model, the sheet resistance should be similar in both heterostructured nanowires and the heterothin films. The calculated sheet resistances were shown in Table I with the comparison to the resistivity data. The sheet resistances are  $1.60 \times 10^{10} (\Omega \text{ sq}^{-1})$  for heterostruc-

TABLE I. Comparison between MgO/NiO heterostructured nanowires and MgO/NiO heterothin films on the resistivity and the sheet resistance data.

	Resistivity ( $\Omega$ cm)	Sheet resistance ( $\Omega$ sq $^{-1}$ )
MgO/NiO heterostructured nanowires	$3.95 \times 10^3$	$1.60 \times 10^{10}$
MgO/NiO heterothin films	$9.37 \times 10^6$	$0.94 \times 10^{10}$

ured nanowires,  $0.94 \times 10^{10}$  ( $\Omega$  sq $^{-1}$ ) for heterothin films, whereas the resistivity data are  $3.95 \times 10^3$  ( $\Omega$  cm) for heterostructured nanowires,  $9.37 \times 10^6$  ( $\Omega$  cm) for heterothin films. Clearly both values of the sheet resistances are comparable, supporting the third model. In addition, we further investigated the thickness dependence of NiO shell layers on the resistivity. If the second model based on the “bulk” effect dominates the transport of heterostructured nanowires, the measured resistivity should be insensitive to the variation of the shell layer thickness. On the other hand, the sheet resistance should be constant even increasing the shell layer thickness if the third model based on the “surface and interface” effect can explain the transport of heterostructured nanowires. Figure 3 shows the thickness dependences on the resistivity and the sheet resistance. It can be clearly seen that the resistivity increased with increasing the shell layer thickness, which is in fact inconsistent with the second model. On the other hand, the calculated sheet resistances were almost constant independent of the shell layer thickness. Thus, these results highlight that the discrepancy between the heterostructured nanowires and the heterothin films on the resistivity in Fig. 2 can be interpreted in terms of the difference of the specific surface area and the surface/interface transport events. Further remained issue is that the major electrical conduction occurs at either “surface” or “interface.” Although we do not have direct experimental evidences to address this issue, there are two indirect implications to support the transport events at the “surface” rather than at “interface.” First, TEM analysis demonstrated the absence of any observable crystal imperfections at the heterointerface.<sup>19</sup> Second, the agreement between the heterostructured nanowires and the heterothin films on the sheet resistances supports the surface effects rather than the heterointerface effects, because in the FPMs the measurable resistance should reflect the transport events mainly at the film surface rather than that at the heterointerface between the film and the substrate.

In summary, we have investigated the transport properties of NiO/MgO heterostructured nanowires by utilizing the noncontact microwave conductivity method. We found the

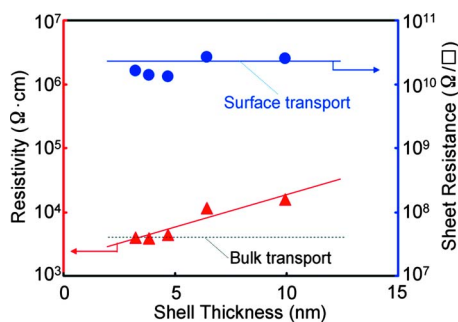


FIG. 3. (Color online) Thickness dependences on the resistivity and the sheet resistance for NiO/MgO heterostructured nanowires.

substantial discrepancy in four orders of magnitude between the NiO heterostructured nanowires and NiO heterothin films on the resistivity when the bulk resistivity tended to increase, whereas such discrepancy was no longer observable for relatively conductive region. The discrepancy between the heterostructured nanowires and thin films on the transport properties can be interpreted in terms of both the large specific surface area of nanowire structures and the surface transport events of insulative NiO. Thus, noncontact microwave transport measurements, performed for at least  $10^{10}$  nanowires in this study, offer statistically reliable transport data of heterostructured nanowires, and would pursue our understanding as to the nanoscale transport events of nanowires by comparing with contact transport measurements of single nanowire.

The authors wish to thank M. Kanai for constructive advice and T. Ishibashi for his invaluable technical support. This work is partially funded by SCOPE.

- <sup>1</sup>K. Xu and J. R. Heath, *Nano Lett.* **8**, 136 (2008).
- <sup>2</sup>T. Yanagida, T. Kanki, B. Vilquin, H. Tanaka, and T. Kawai, *Phys. Rev. B* **70**, 184437 (2004).
- <sup>3</sup>W. Eerenstein, M. Wiora, J. L. Prieto, J. F. Scott, and N. D. Mathur, *Nature Mater.* **6**, 348 (2007).
- <sup>4</sup>R. Waser and M. Aono, *Nature Mater.* **6**, 833 (2007).
- <sup>5</sup>K. Nagashima, T. Yanagida, H. Tanaka, and T. Kawai, *J. Appl. Phys.* **101**, 026103 (2007).
- <sup>6</sup>C. M. Lieber and Z. L. Wang, *MRS Bull.* **32**, 99 (2007).
- <sup>7</sup>R. Newman and R. M. Chrenko, *Phys. Rev.* **114**, 1507 (1959).
- <sup>8</sup>J. McCord, R. Kaltofen, T. Gemming, R. Hühne, and L. Schultz, *Phys. Rev. B* **75**, 134418 (2007).
- <sup>9</sup>A. K. M. S. Chowdhury, S. A. Akbar, S. Kapileshwar, and J. R. Schorr, *J. Electrochem. Soc.* **148**, G91 (2001).
- <sup>10</sup>H. Kamal, E. K. Elmaghraby, S. A. Ali, and K. Abdel-Hady, *Thin Solid Films* **483**, 330 (2005).
- <sup>11</sup>K. Kinoshita, T. Tamura, M. Aoki, Y. Sugiyama, and H. Tanaka, *Appl. Phys. Lett.* **89**, 103509 (2006).
- <sup>12</sup>I. K. Yoo, B. S. Kang, Y. D. Park, M. J. Lee, and Y. Park, *Appl. Phys. Lett.* **92**, 202112 (2008).
- <sup>13</sup>J. Y. Son and Y.-H. Shin, *Appl. Phys. Lett.* **92**, 222106 (2008).
- <sup>14</sup>Y. Lin, T. Xie, B. Cheng, B. Geng, and L. Zhang, *Chem. Phys. Lett.* **380**, 521 (2003).
- <sup>15</sup>S. I. Kim, J. H. Lee, Y. W. Chang, S. S. Hwang, and K. H. Yoo, *Appl. Phys. Lett.* **93**, 033503 (2008).
- <sup>16</sup>S. Han, C. Li, Z. Liu, B. Lei, D. Zhang, W. Jin, X. Liu, T. Tang, and C. Zhou, *Nano Lett.* **4**, 1241 (2004).
- <sup>17</sup>D. Zhang, Z. Liu, S. Han, C. Li, B. Lei, M. P. Stewart, J. M. Tour, and C. Zhou, *Nano Lett.* **4**, 2151 (2004).
- <sup>18</sup>C. Li, B. Lei, Z. Luo, S. Han, Z. Liu, D. Zhang, and C. Zhou, *Adv. Mater.* **17**, 1548 (2005).
- <sup>19</sup>K. Oka, T. Yanagida, K. Nagashima, H. Tanaka, and T. Kawai, *J. Am. Chem. Soc.* **131**, 3434 (2009).
- <sup>20</sup>K. Nagashima, T. Yanagida, H. Tanaka, S. Seki, A. Saeki, S. Tagawa, and T. Kawai, *J. Am. Chem. Soc.* **130**, 5378 (2008); A. Marcu, T. Yanagida, K. Nagashima, K. Oka, H. Tanaka, and T. Kawai, *Appl. Phys. Lett.* **92**, 173119 (2008).
- <sup>21</sup>K. Nagashima, T. Yanagida, H. Tanaka, and T. Kawai, *Appl. Phys. Lett.* **90**, 233103 (2007); *J. Appl. Phys.* **101**, 124304 (2007); A. Marcu, T. Yanagida, K. Nagashima, H. Tanaka, and T. Kawai, *ibid.* **102**, 016102 (2007); T. Yanagida, K. Nagashima, H. Tanaka, and T. Kawai, *Appl. Phys. Lett.* **91**, 061502 (2007); T. Yanagida, K. Nagashima, H. Tanaka, and T. Kawai, *J. Appl. Phys.* **104**, 016101 (2008); K. Nagashima, T. Yanagida, K. Oka, H. Tanaka, and T. Kawai, *Appl. Phys. Lett.* **93**, 153103 (2008); T. Yanagida, A. Marcu, H. Matsui, K. Nagashima, K. Oka, K. Yokota, M. Taniguchi, and T. Kawai, *J. Phys. Chem. C* **112**, 18923 (2008).
- <sup>22</sup>Y. Yamamoto, T. Fukushima, Y. Suna, N. Ishii, A. Saeki, S. Seki, S. Tagawa, M. Taniguchi, T. Kawai, and T. Aida, *Science* **314**, 1761 (2006).
- <sup>23</sup>K. Oka, T. Yanagida, K. Nagashima, H. Tanaka, and T. Kawai, *J. Appl. Phys.* **104**, 013711 (2008).
- <sup>24</sup>W. E. Spear and D. S. Tannhauser, *Phys. Rev. B* **7**, 831 (1973).
- <sup>25</sup>C. H. Olk, S. M. Yalisove, and G. L. Doll, *Phys. Rev. B* **52**, 1692 (1995).